IEEE Access
Multidisciplinary ⋮ Rapid Review ⋮ Open Access Journal

Received October 29, 2020, accepted November 9, 2020, date of publication November 16, 2020, date of current version November 23, 2020.

Digital Object Identifier 10.1109/ACCESS.2020.3037816

Neural Membrane Mutual Coupling Characterisation Using Entropy-Based Iterative Learning Identification

XIAFEI TANG[1], QICHUN ZHANG[2], (Senior Member, IEEE), XUEWU DAI[3], (Member, IEEE), AND YIQUN ZOU[4]

[1]Engineering Research Center of the Ministry of Education (Power Grid Security Monitoring and Control Technology), Changsha University of Science and Technology, Changsha 410114, China
[2]Department of Computer Science, University of Bradford, Bradford BD7 1DP, U.K.
[3]Department of Mathematics, Physics and Electrical Engineering, Northumbria University, Newcastle upon Tyne NE1 8QH, U.K.
[4]School of Automation, Central South University, Changsha 410083, China

Corresponding author: Qichun Zhang (q.zhang17@bradford.ac.uk)

This work was supported in part by the National Natural Science Foundation of China (NSFC) under Grant 51807010, and in part by the Natural Science Foundation of Hunan under Grant 1541 and Grant 1734.

ABSTRACT This paper investigates the interaction phenomena of the coupled axons while the mutual coupling factor is presented as a pairwise description. Based on the Hodgkin-Huxley model and the coupling factor matrix, the membrane potentials of the coupled myelinated/unmyelinated axons are quantified which implies that the neural coupling can be characterised by the presented coupling factor. Meanwhile the equivalent electric circuit is supplied to illustrate the physical meaning of this extended model. In order to estimate the coupling factor, a data-based iterative learning identification algorithm is presented where the Rényi entropy of the estimation error has been minimised. The convergence of the presented algorithm is analysed and the learning rate is designed. To verified the presented model and the algorithm, the numerical simulation results indicate the correctness and the effectiveness. Furthermore, the statistical description of the neural coupling, the approximation using ordinary differential equation, the measurement and the conduction of the nerve signals are discussed respectively as advanced topics. The novelties can be summarised as follows: 1) the Hodgkin-Huxley model has been extended considering the mutual interaction between the neural axon membranes, 2) the iterative learning approach has been developed for factor identification using entropy criterion, and 3) the theoretical framework has been established for this class of system identification problems with convergence analysis.

INDEX TERMS Neural coupling analysis, extended Hodgkin-Huxley model, equivalent electric circuit, information entropy, iterative learning, convergence analysis, statistical description, kernel density estimation.

I. INTRODUCTION

The interaction widely exists between the axons in nerve fibres. For example, the ephaptic interaction phenomena is known to exist in vivo and is not insignificant [1]. However, most of the existing results did not investigate the coupling problem or ignore this interaction. Basically, most of the existing results have been developed based on the well-known Hodgkin-Huxley model [2]. Almost all of these results, such as Frankenhaeuser-Huxley model [3], focus on the response of the individual axons in order to describe the mechanism of the membrane potential. On the other hand, the neural coupling in brain is investigated in [4] however these coupling analysis is mostly about the cognitive- emotional-based without the mechanism description in neural-electrical sense. Moreover, the neuron and electrode interaction has been considered in [5] where an equivalent electric circuit is developed. This circuit is difficult to extend to multi-axon nerve fibres and no approach is taken into account for the parameter identification in this circuit. Similarly, a mathematical study of the nerve fibre interaction is given in [6] in simplified geometrical format which is also difficult to generalise.

The associate editor coordinating the review of this manuscript and approving it for publication was Shuping He.

Is it possible to use a similar mechanism descriptive approach to characterise these couplings between peripheral nerve axons? Tying to answer this question forms the purpose of this paper.

There is no existing solution to characterise these couplings which is the main challenge of this research. Therefore, the mutual coupling factor is presented in this paper to describe the axon-to-axon interaction which means that the neural couplings can be characterised if the mutual coupling factor can be estimated. However, due to the strong nonlinearity and randomness, the identification problem is very difficult to solve even the description of the interaction can be introduced by coupling factors. Although some algorithms are given in [7], these algorithms cannot be applied directly. Motivated by the iterative learning control [8]–[10], the iterative learning identification [11], [12] can be considered as a possible approach to achieve the objective where the batch-based information can be used to overcome the nonlinearity of the model. Notice that the challenge of this research also brings the benefits not only for the theoretical research but also for the neural applications. Based on the presented characterisation, the interaction can be analysed using the numerical approach and the performance of the neural applications can be enhanced, such as neural prosthesis design and development [13], [14].

Following the discussion above, the contents and the novelties of this paper can be summarised as follows: At first, a descriptive model for the interaction between the coupled axons has been presented which is motivated by the Hodgkin-Huxley equation. The mutual coupling factor matrix has been introduced into this model which can be adopted as an extension of any exiting membrane potential models. Based upon this approach, the couplings can be described and characterised once the mutual coupling factor is known. Secondly, a data-based iterative learning identification algorithm is presented to estimate the mutual coupling factors if these factors are unknown, where the entropy-based performance criterion is proposed. Information entropy is a mathematical description of the randomness which is widely used for performance optimisation [15], [16] and filtering design [17], [18]. To verify and analyse this presented algorithm, the convergence has been demonstrated by both numerical simulation and analytic proof. As the last part of this paper, the further discussions are given. The statistical description of the interaction is briefly introduced using the similar approach. The measurement, conduction and simplified approximation of the nerve signals are presented via measurement equation, partial differential equation (PDE) and ordinary differential equation (ODE), respectively.

Then the rest of this paper is organised as follows: In Section II, a simplified example is given to illustrate the interaction between two coupled axons using the conductance and Hodgkin-Huxley model, which leads to the equivalent electric circuit. Following the this description, the generalised extended Hodgkin-Huxley model has been presented for n coupled axons, where the mutual coupling factor has been introduced as the characterisation of the neural interaction. The entropy-based iterative learning algorithm is presented in Section III. Particularly, the performance criterion, algorithm procedure and convergence analysis are given in this section. Section IV shows the numerical simulation results based on the presented model and algorithm. All these results indicate that the presented algorithm can be applied to find out the mutual coupling factor and further characterise the axon-to-axon couplings. Some useful discussions are given in Section V. In the end, Section VI concludes the novelties and contributions of this paper.

There are some symbols will be used in the modelling and identification, therefore the key symbols are demonstrated by Table 1 in order to enhance the readability of the paper.

TABLE 1. Table of key symbols.

V_m	Membrane potential
V_{out}	External membrane potential
V_{in}	Internal membrane potential
V_r	Resting potential of neuron
V	Membrane potential vector
$\tilde{V}$	Membrane potential estimation error
I_{ion}	Current of ionic channel
I	Membrane current
g	Conductance
C_m	Capacitance
G_a	Internodal axial conductance
Ξ	Coupling factor matrix
e_k	Measurement uncertainty
t_s	Sampling time
k	Discretisation index
d	Batch index
Δs	Compartment length
ϵ	Escape factor
γ	Coupling factor
ε_d	Step of the gradient descent
$\mathscr{E}(\cdot)$	Mean-value operator
$\mathscr{H}(\cdot)$	Entropy operator
$\mathscr{P}(\cdot)$	Information potential operator
$G_\sigma(\cdot)$	Gaussian kernel function

II. EXTENDED HODGKIN-HUXLEY MODEL

A. A SIMPLIFIED DESCRIPTION OF TWO COUPLED AXONS

The simplest situation of the neural interaction can be described by two different membranes which belong to two nearby coupled axons. Ignoring connective/interstitial tissue for now, the extracellular space between these two axons can be described as a simple conductance. Therefore the interaction current would be driven by the voltage between the respective external membrane potentials. Combining the Hodgkin-Huxley model with this interaction description, the model of two coupled membranes can be obtained as follows:

$$\begin{aligned} c_{m_1}\frac{\partial V_{m_1}}{\partial t} &= -I_{ion_1} - g_{12}\left(V_{out_1} - V_{out_2}\right) \\ c_{m_2}\frac{\partial V_{m_2}}{\partial t} &= -I_{ion_2} - g_{21}\left(V_{out_2} - V_{out_1}\right) \end{aligned} \tag{1}$$

where V_m denotes the membrane potential, g stands for the conductance and V_{out} is the external membrane potential.

Note that $g_{12} = g_{21}$, while the I_{ion} is the current of the potassium, sodium and leakage channels. Moreover, the currents of ionic channels can be further expressed by the following equations:

$$I_{ion_i} = I_{Na,i} + I_{Ka,i} + I_{leak,i}, i = 1, 2 \tag{2}$$

where

$$\begin{aligned} I_{Na,i} &= m_i^3 \left(V_{m_i}, t\right) h_i \left(V_{m_i}, t\right) \bar{g}_{Na} \left(V_{m_i} - V_{Na}\right) \\ I_{Ka,i} &= n_i^4 \left(V_{m_i}, t\right) \bar{g}_{Ka} \left(V_{m_i} - V_{Na}\right) \\ I_{leak,i} &= \bar{g}_{leak} \left(V_{m_i} - V_{leak}\right) \end{aligned} \tag{3}$$

Notice that n, m and h are non-linear functions of V_m and time t which is illustrated in [2]. The model can be extended to n axons based on the two-axon form. However, the interaction is mutual and we can combine multi-axon into one virtual axon [19], then we use two-axon model in this paper to indicate the methodology without loss of generality.

B. THE EQUIVALENT ELECTRIC CIRCUIT

The equivalent electric circuit is illustrated by Fig.1 for three axons, for generality. Based on the above discussion for two coupled membranes, it has been shown that the conductance exists between each two coupled axons. Then it can be claimed that these interactions can be generalised using the pairwise description, in other words, the neural coupling of the axons can be further characterised by the format of symmetric conductance matrix.

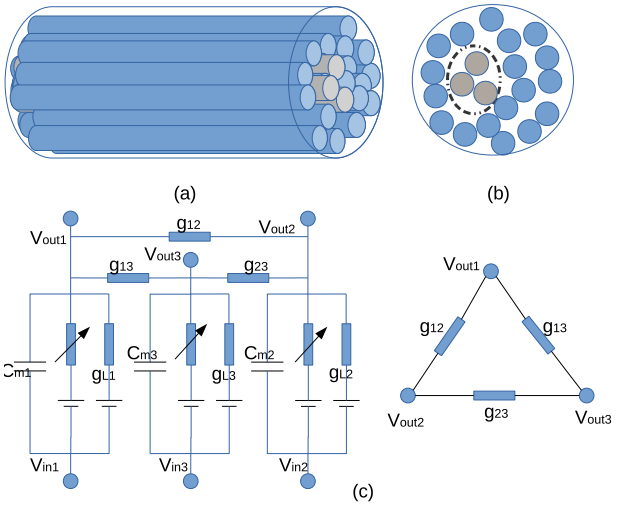

FIGURE 1. The description of the extended membrane model with interaction. (a)The chosen three coupled axons in the multi-axons nerve fibres; (b)The simplified transverse diagram according to (a); (c)The equivalent electrical circuit with mutual coupling factors for 3 coupled axons based on Hodgkin-Huxley model.

Note that the conductance matrix in this equivalent electric circuit is considered as real constants which means that the dynamic of the interaction has been neglected and the conductance is time-invariant.

C. GENERALISED COUPLING DESCRIPTION OF n AXONS

Based upon the presented extended Hodgkin-Huxley model, the generalised model can be obtained naturally for n coupled membranes using the pairwise conductance. Therefore, the generalised model for n coupled membranes is given as follows:

$$\begin{aligned} c_{m_1} \frac{\partial V_{m_1}}{\partial t} &= -I_{ion_1} - \sum_{j=1}^{n} g_{1j} \left(V_{out_1} - V_{out_j}\right) \\ &\vdots \\ c_{m_n} \frac{\partial V_{m_n}}{\partial t} &= -I_{ion_n} - \sum_{j=1}^{n} g_{nj} \left(V_{out_n} - V_{out_j}\right) \end{aligned} \tag{4}$$

Thus, the model can be further rewritten in the following compact form using the vector expression:

$$\dot{V} = \bar{C} \left(-\bar{I} - \Xi V_{out}\right) \tag{5}$$

where

$$V = \left[V_{m_1}, \ldots, V_{m_n}\right]^T$$

$$V_{out} = \left[V_{out_1}, \ldots, V_{out_n}\right]^T$$

$$\bar{I} = \left[I_{ion_1}, \ldots, I_{ion_n}\right]^T \tag{6}$$

$$\bar{C} = diag\left\{\frac{1}{c_{m_1}}, \ldots, \frac{1}{c_{m_n}}\right\} \tag{7}$$

$$\Xi = \begin{bmatrix} \gamma_1 & -g_{12} & \cdots & -g_{1n} \\ * & \gamma_2 & \cdots & -g_{2n} \\ \vdots & \vdots & \ddots & \vdots \\ * & * & \cdots & \gamma_n \end{bmatrix} \tag{8}$$

with $\gamma_i = \sum_{j=1}^{n} g_{ij} - g_{ii}, i = 1, \ldots, n.$

Notice that Ξ can be further used to characterise the coupling, then we can define Ξ as the mutual coupling factor matrix where $*$ denotes the symmetric element.

Moreover, the relationship between the external membrane potential and the trans-membrane potential can be given by the following definition.

$$V = V_{in} - V_{out} \tag{9}$$

where V_{in} denotes the internal membrane potential.

Due to the fact that the internal membrane potential is dominated by the applied stimulation current I_{ap}, we can claim that there exists a non-linear function as follows:

$$V_{in} = f\left(V, I_{ap}\right) \tag{10}$$

Thus, the complete description of the mutual interaction between the coupled nerve fibres is as follows:

$$\dot{V} = \bar{C} \left(-\bar{I} - \Xi f\left(V, I_{ap}\right) + \Xi V\right) \tag{11}$$

Furthermore, to simplify the expression, this model above can be expressed as a general non-linear differential equation with V_m, Ξ and I_{ap}.

$$\dot{V} = \bar{f}\left(V, \Xi, I_{ap}\right) \tag{12}$$

Based on Eq.(12), the coupling can be characterised by the mutual coupling factor Ξ identification using the experimental data of V_m and I_{ap}. Since the experimental data set is always described by discrete point set, the discrete-time format of Eq.(12) can be approximated by

$$V_k = V_{k-1} + t_s \bar{f}\left(V_{k-1}, \Xi, I_{ap}\right) \tag{13}$$

where k and t_s stand for the sampling index and sampling time, respectively.

Remark 2.1: The current exchange causes the interactions between the axons, where we suppose that the escape current can be ignored then the current from axon one will fully transmit to axon two. As a result, it can be described as a symmetric form in the formulation.

III. COUPLING CHARACTERISATION

A. ENTROPY-BASED PERFORMANCE EVALUATION

Basically, we can characterise the interaction for n coupled axons if the membrane potential signals of these n individual axons can be measured and collected. In practice, the measurement noise cannot be avoided once the electrode interface has been taken into accounts, then the measured membrane potential can be formulated by

$$\bar{V}_k = V_k + e_k \tag{14}$$

where e denotes the error and the noise of the measurement. Note that it is impossible to accurately model all the axons in the nerve fibres therefore the measured signal of n axons would be affected by some other un-modelled axons. These influences cannot be treated as the disturbance then we conclude them as the error of the measurement.

Suppose that the initial value of the mutual coupling factor is selected properly as $\hat{\Xi}$, then the estimated measured membrane potential can be expressed as

$$\hat{\bar{V}}_k = \hat{\bar{V}}_{k-1} + t_s \bar{f}\left(\hat{\bar{V}}_{k-1}, \hat{\Xi}, I_{ap}\right) \tag{15}$$

Comparing to the actual measured data, the estimated error can be further expressed by

$$\tilde{V}_k\left(\hat{\Xi}\right) = \bar{V}_k - \hat{\bar{V}}_k\left(\hat{\Xi}\right) \tag{16}$$

Actually, the initial value of $\hat{\Xi}$ can be selected as any real matrix however a proper initialisation can reduce the time of identification.

Note that we can obtain a data set of the estimated error with k elements if we consider this operation as one batch.

$$\tilde{V}_d\left(\hat{\Xi}_d\right) = \left[\tilde{V}_{d,1}^T\left(\hat{\Xi}_d\right), \ldots, \tilde{V}_{d,k}^T\left(\hat{\Xi}_d\right)\right]^T, \quad d = 1 \tag{17}$$

Similarly, we can have d batches of the data set if we repeat this operation for d times. Therefore, the objective of this algorithm is to find out the optimal coupling factor matrix $\hat{\Xi}_d$ to minimise the estimated error using the data vector with d-th batch.

Since the data set is a vector with the error and zero-mean noise of the measurement, the statistical performance criterion is considered as the cost function, however this error data set cannot be assumed to obey Gaussian distribution. Due to the nonlinearity of the mutual couplings among the axons, the distribution of the measured membrane potentials will be non-Gaussian variables which leads that the estimation error sets would also be non-Gaussian. Therefore, motivated by [20], we use the following mathematical expectation and quadratic Rényi entropy criterion [21] to deal with the possible non-Gaussian stochastic distribution.

$$J_d = \mathscr{E}\left(\tilde{V}_d^T\left(\hat{\Xi}_d\right)\tilde{V}_d\left(\hat{\Xi}_d\right)\right) + \mathscr{H}\left(\tilde{V}_d\left(\hat{\Xi}_d\right)\right) \tag{18}$$

where

$$\mathscr{H}\left(\tilde{V}_d\left(\hat{\Xi}_d\right)\right) = -\log_b \int \gamma_d^2\left(\alpha_d\right) d\alpha_d \tag{19}$$

while γ_d and α_d denote the probability density function of the d-th batch estimated error set and the random variable of this data set, respectively. In particular, the entropy is equivalent to variance for the Gaussian random variable and the associate probability density function will become sharper with the attenuation of the entropy [22].

Based on the concept of the information potential [21], the performance criterion above can be rewritten as the following expression if the base of the logarithm function is selected as $0 < b < 1$.

$$J_d = \mathscr{E}\left(\tilde{V}_d^T\left(\hat{\Xi}_d\right)\tilde{V}_d\left(\hat{\Xi}_d\right)\right) + \mathscr{P}\left(\tilde{V}_d\left(\hat{\Xi}_d\right)\right) \tag{20}$$

where the information potential is given as

$$\mathscr{P}\left(\tilde{V}_d\left(\hat{\Xi}_d\right)\right) = \int \gamma_d^2\left(\alpha_d\right) d\alpha_d \tag{21}$$

Since the selected logarithm function is monotone decreasing function, the minimum can be obtained if the transformed performance criterion is minimised.

B. ITERATIVE LEARNING IDENTIFICATION

Next, the iterative learning approach is applied to estimate the coupling factor matrix Ξ based on the collected data and the presented model.

$$\hat{\Xi}_d = \hat{\Xi}_{d-1} - \varepsilon_d \frac{dJ_{d-1}}{d\Xi_d}\bigg|_{\Xi_d = \hat{\Xi}_{d-1}} \tag{22}$$

where $\varepsilon_d > 0$ stands for the step of the gradient descent. Thus the identification strategy can be illustrated by Fig. 2. Basically, the step is also the learning rate of the iterative algorithm, the ε_d should be chosen properly to guarantee the convergence of the iterative learning algorithm which is going to be analysed in the next subsection.

In practice, the derivative can be replaced by the difference then the formula can be rewritten as

$$\hat{\Xi}_d = \hat{\Xi}_{d-1} - \varepsilon_d \frac{J_{d-1} - J_{d-2}}{\hat{\Xi}_{d-1} - \hat{\Xi}_{d-2}}, \quad s.t. \left\| \hat{\Xi}_{d-1} - \hat{\Xi}_{d-2} \right\| \geq \delta \tag{23}$$

where $\delta > 0$ denotes the pre-specified threshold.

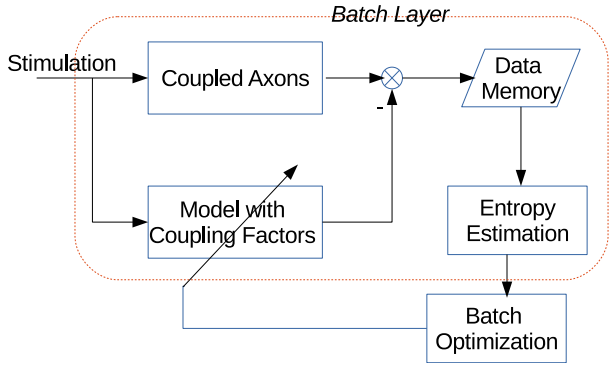

FIGURE 2. Block diagram of the presented iterative learning strategy.

Note that the probability density function can be estimated by the data directly using the kernel density estimation [23] as follows.

$$\hat{\gamma}_d = \frac{1}{k\bar{h}} \sum_{i=1}^{nk} G_\sigma \left(\frac{\alpha_d - \tilde{V}_{d,i}}{\bar{h}} \right) \tag{24}$$

where $\tilde{V}_{d,i}$ denotes the signal element of the vector $\tilde{V}_d$. Based upon this approximation, the information potential can also estimated by

$$\mathscr{P}\left(\tilde{V}_d\left(\hat{\Xi}_d\right)\right) = \frac{1}{(k\bar{h})^2} \sum_{i=1}^{nk} \left[\sum_{j=1}^{nk} G_\sigma \left(\frac{\tilde{V}_{d,j} - \tilde{V}_{d,i}}{\bar{h}} \right) \right]^2 \tag{25}$$

Thus, the value of the performance criterion can be calculated for each batch, where G_σ and $\bar{h}$ denote the Gaussian kernel function and bin width, respectively. Particularly, G_σ is selected as follows.

$$G_\sigma(x) = \frac{1}{\sqrt{2\pi}} \exp\left(\frac{-x^2}{2\sigma^2} \right) \tag{26}$$

C. ALGORITHM ANALYSIS

Before the presented algorithm is implemented, the essential analysis has to be given where the most important analysis should be the convergence of the presented algorithm.

It has been shown that the performance criterion is formed by mean value and the entropy where the entropy is approximated by kernel density estimation. Then we firstly analyse the sub performance criterion only with entropy, which can be expressed as follows:

$$J_{sub,d} = \mathscr{H}\left(\tilde{V}_d\left(\hat{\Xi}_d\right)\right) \tag{27}$$

Based on the kernel density estimation and this sub performance criterion, the following Lemma can be obtained.

Lemma 3.1: Using the sub performance criterion (27) and the iterative learning formula (22), the convergence can be guaranteed if there exists a learning rate ε_d such that the following sign equation holds.

$$sign(\varepsilon_d) = -sign\left(\sup\left(\tilde{V}_{d-1}\right) \sup\left(\frac{\partial J_{d-1}}{\partial \Xi_{d-1}} \right) \right) \tag{28}$$

where *sign* denotes the sign function.

Proof: This proof is given in Appendix A. ■

Similar to Lemma 3.1, let's consider the mean value part of the performance criterion as the sub performance criterion.

$$J_{sub,d} = \mathscr{E}\left(\tilde{V}_d^T\left(\hat{\Xi}_d\right)\tilde{V}_d\left(\hat{\Xi}_d\right)\right) \tag{29}$$

Then the following lemma can be obtained.

Lemma 3.2: Using the sub performance criterion (29) and the iterative learning formula(22), the convergence can be guaranteed if there exists a learning rate ε_d such that the following inequality can be satisfied.

$$\bar{A}_d \varepsilon_d^T \varepsilon_d + 2\bar{B}_d \varepsilon_d + \bar{C}_d < 0 \tag{30}$$

where the coefficients are defined as follows:

$$\bar{A}_d = t_s^2 \bar{C}^T \bar{C} \sum_{j=1}^{k-1} \sum_{i=1}^{j} \left(\left(\frac{dJ_{d-1}}{d\Xi_{d-1}} \left(f_{d,i} - V_{d,i}\right) \right)^T \times \frac{dJ_{d-1}}{d\Xi_{d-1}} \left(f_{d,i} - V_{d,i}\right) \right) \tag{31}$$

$$\begin{aligned} \bar{B}_d = {} & t_s^2 \bar{C}^T \bar{C} I_{d,i}^T \sum_{j=1}^{k-1} \sum_{i=1}^{j} \left(\frac{dJ_{d-1}}{d\Xi_{d-1}} \left(V_{d,i} - f_{d,i}\right) \right) \\ & - t_s \hat{\bar{V}}_{d,1}^T \bar{C} \sum_{j=1}^{k-1} \sum_{i=1}^{j} \left(\frac{dJ_{d-1}}{d\Xi_{d-1}} \left(V_{d,i} - f_{d,i}\right) \right) \\ & - t_s \bar{C} \sum_{j=1}^{k-1} \sum_{i=1}^{j} \bar{V}_{j+1}^T \left(\frac{dJ_{d-1}}{d\Xi_{d-1}} \left(f_{d,i} - V_{d,i}\right) \right) \\ & - t_s^2 \bar{C}^T \bar{C} \sum_{j=1}^{k-1} \sum_{i=1}^{j} \left(\left(f_{d,i} - V_{d,i}\right)^T \times \frac{dJ_{d-1}}{d\Xi_{d-1}} \Xi_{d-1} \left(f_{d,i} - V_{d,i}\right) \right) \end{aligned} \tag{32}$$

$$\begin{aligned} \bar{C}_d = {} & t_s^2 \bar{C}^T \bar{C} \sum_{j=1}^{k-1} \sum_{i=1}^{j} \left(\bar{I}_{d,i}^T \bar{I}_{d,i} + 2 I_{d,i}^T \Xi_{d-1} \left(f_{d,i} - V_{d,i}\right) \right) \\ & - 2 t_s \hat{\bar{V}}_{d,1}^T \bar{C} \sum_{j=1}^{k-1} \sum_{i=1}^{j} \left(\bar{I}_{d,i} + \Xi_{d-1} \left(f_{d,i} - V_{d,i}\right) \right) \\ & + t_s^2 \bar{C}^T \bar{C} \sum_{j=1}^{k-1} \sum_{i=1}^{j} \left(\left(f_{d,i} - V_{d,i}\right)^T \bar{\Xi} \left(f_{d,i} - V_{d,i}\right) \right) \\ & - 2 t_s \bar{C} \sum_{j=1}^{k-1} \sum_{i=1}^{j} \bar{V}_{j+1}^T \left(\bar{I}_{d-1,i} + \Xi_{d-1} \left(f_{d-1,i} - V_{d-1,i}\right) \right. \\ & \left. - \bar{I}_{d,i} - \Xi_{d-1} \left(f_{d,i} - V_{d,i}\right) \right) + k \hat{\bar{V}}_{d,1}^T \hat{\bar{V}}_{d,1} \end{aligned} \tag{33}$$

while $\bar{\Xi} = \Xi_{d-1}^T \Xi_{d-1}$.

Proof: This proof is given in Appendix B. ■

Replacing the sub performance criterion by the presented performance criterion, the following theorem is given.

Theorem 3.3: Using the iterative learning identification(22), the convergence of the estimated mutual coupling factor can be guaranteed if there exists a learning rate ε_d such that conditions (28) and (30) can be satisfied.

Proof: For any d-batch, the presented iterative learning identification algorithm is convergent if the following inequality hold.

$$J_d - J_{d-1} < 0 \tag{34}$$

which implies that the performance criterion strictly decrease with the increase of the iteration.

Substituting the formula of the performance criterion, we have

$$\mathscr{E}\left\{\tilde{V}_d^T\left(\hat{\Xi}_d\right)\tilde{V}_d\left(\hat{\Xi}_d\right) - \tilde{V}_{d-1}^T\left(\hat{\Xi}_{d-1}\right)\tilde{V}_{d-1}\left(\hat{\Xi}_{d-1}\right)\right\} + \mathscr{P}\left(\tilde{V}_d\left(\hat{\Xi}_d\right)\right) - \mathscr{P}\left(\tilde{V}_{d-1}\left(\hat{\Xi}_{d-1}\right)\right) < 0 \tag{35}$$

Note that this inequality condition can be satisfied if the following two inequalities hold at the same time.

$$\tilde{V}_d^T\left(\hat{\Xi}_d\right)\tilde{V}_d\left(\hat{\Xi}_d\right) - \tilde{V}_{d-1}^T\left(\hat{\Xi}_{d-1}\right)\tilde{V}_{d-1}\left(\hat{\Xi}_{d-1}\right) < 0 \tag{36}$$

$$\mathscr{P}\left(\tilde{V}_d\left(\hat{\Xi}_d\right)\right) - \mathscr{P}\left(\tilde{V}_{d-1}\left(\hat{\Xi}_{d-1}\right)\right) < 0 \tag{37}$$

Note that the second inequality holds if the sign of the learning rate ε_d can be selected by Lemma 3.2 due to the equivalence of the information potential criterion and entropy criterion. Meanwhile the first inequality can be satisfied directly by Lemma 3.1. Therefore the proof is completed combining the conditions of the presented Lemmas. ■

Based on this analysis, the procedure of the presented iterative learning algorithm can be illustrated by the following flow chart.

Remark 3.1: If we only have the measured data set, the dimension of the model should be confirmed before estimating mutual coupling factor, i.e. the number of the axons in the model. The optimal dimension can be approximated following mutual information criterion [24], however we can characterise the interaction even if the dimension of the model is improper. The characterisation would be reflected by the value of the estimated mutual coupling factor which would be affected by the pre-specified number of the axons in the model.

Remark 3.2: In practice, as the step is fixed for each batch, the selection of the step can be small for the initial value. Then the convergence can be guaranteed for re-selection following condition (30). Otherwise, the unconverging batch can be abandoned.

IV. NUMERICAL SIMULATIONS

A. NEURAL COUPLING DEMONSTRATIONS

To verify the performance of the presented model, a numerical simulation is given in this section. Firstly, we choose the standard Hodgkin-Huxley model with the appropriate parameters [2]. Without loss of generality, we considered the simulation as three axons while the membrane potentials of these axons are denoted by V_{m_1}, V_{m_2} and V_{m_3}. The objective is to show the responses of the coupled axons when we stimulate only one of the axons. Note that the simulation is based on the non-clinical data, where the key point of this section is to validate the presented identification algorithm.

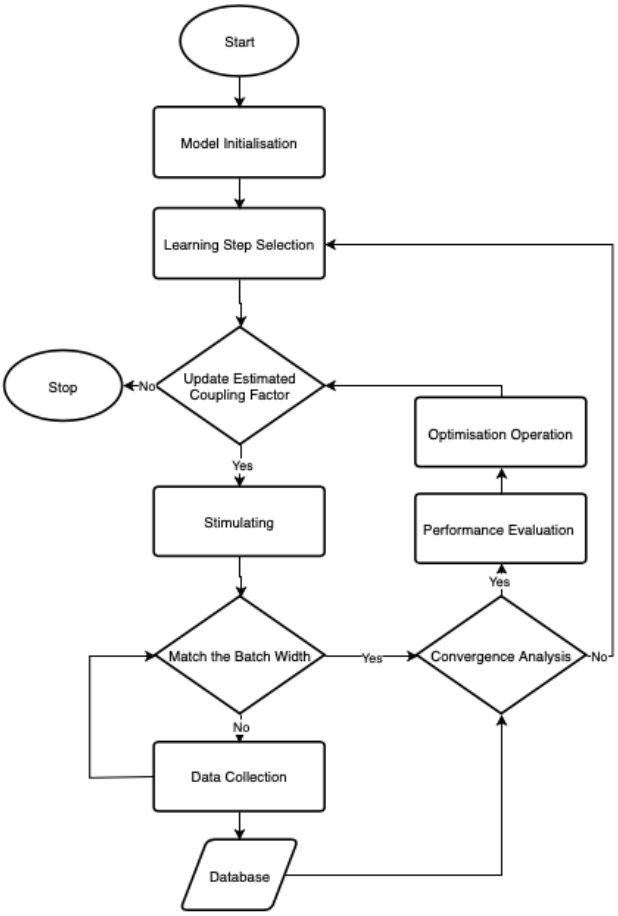

FIGURE 3. The flow chart for the presented iterative learning identification algorithm.

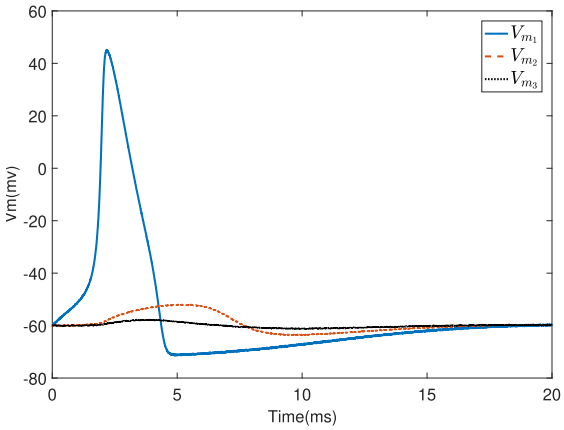

FIGURE 4. The responses of the coupled axons.

To start the simulation, the stimulus is set as an intracellular current density of $0.1mA/cm^2$ and the duration is 0.2 ms, which is similar to the settings in [25]. When this stimulus is applied to axon 1, the responses of axon 2 an axon 3 are shown in the following figure, while the mutual coupling factors are selected as $g_{12} = 0.00055$, $g_{13} = 0.0002$ and $g_{23} = 0.0005$.

From Fig.4, it is clear that if the coupling factor is small, which means that axon 1 has a very small effect on axon 2,

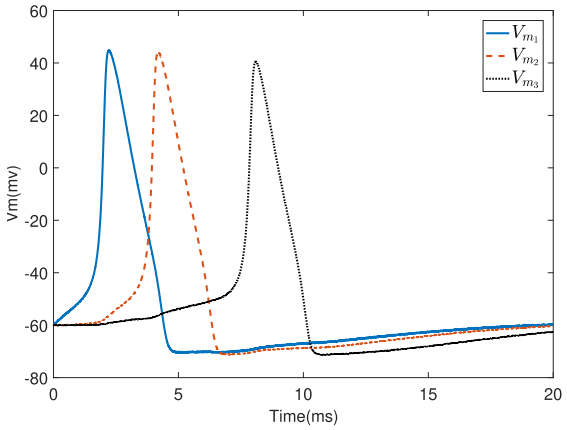

FIGURE 5. The responses of the coupled axons.

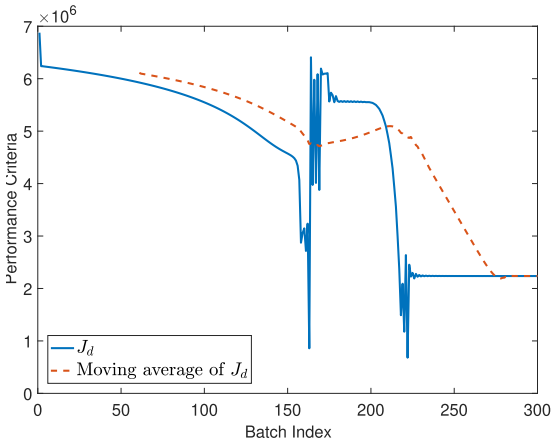

FIGURE 7. The decrease of the performance criterion.

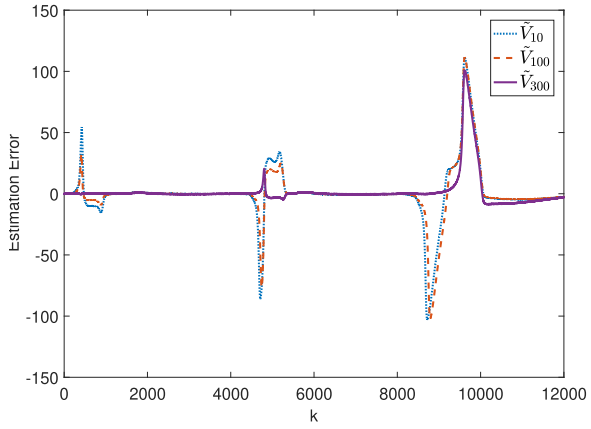

FIGURE 6. The error curves of the estimation for 4 different batches.

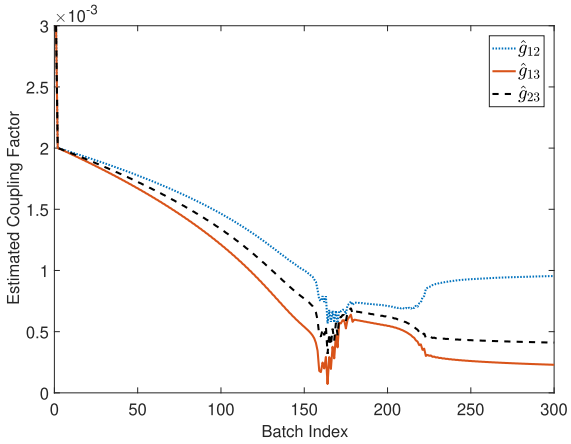

FIGURE 8. The batch-based estimated mutual coupling factor.

then axon 2 cannot produce an action potential. If the coupling factor $g_{12} = 0.001$, Fig.5 indicates that the action potential can be formed if the coupling factor is big enough even if there is no artificial stimuli on axon 2 and 3.

B. COUPLING FACTOR IDENTIFICATION

Following the simulation results above, a simple example is investigated as a numerical illustration where three coupled axons are considered. Then, as the main result of this section, the iterative learning algorithm is applied for a known Hodgkin-Huxley model with a fixed coupling factor matrix $g_{12} = 0.001$, $g_{13} = 0.0002$ and $g_{23} = 0.0005$. Based upon the presented algorithm, the error data of the estimation can be collected for each batch, which is shown in Fig. 6 and the associate value of the performance criterion is demonstrated by Fig. 7. Both of these results show that the presented identification algorithm is convergent for the interaction characterisation. In the end, Fig. 8 the curve of the estimated coupling factor shows that the estimated coupling factors are very close to the pre-specified coupling factors.

Using this numerical example, we validate the presented algorithm. In practice, the neural interaction among axons can be characterised following this algorithm with the measured experimental data.

In particular, the results of using least-square method have been demonstrated in [26] as a comparison. The investigated model is of strong non-linearity, the coupling factor identification is sensitive based on the real-time data process. Alternatively, we can use evolutionary algorithms and deep learning network to train the model which lead to the good results if the computational workload can be ignored. Furthermore, these algorithms cannot guarantee the convergence in theory sense. The presented algorithm considered the characteristics of the axon membrane and the theoretical analysis has been developed in terms of convergence which is different from other data-based evolutionary algorithm and AI algorithms.

V. DISCUSSIONS

A. THE MEASUREMENT OF NERVE SIGNALS

It is very difficult to measure each individual axons, mostly the neural signal data we collected is the integral of many axons. Considering the measurement techniques, such as voltage/current clamping [27], extracellular electrode [28],

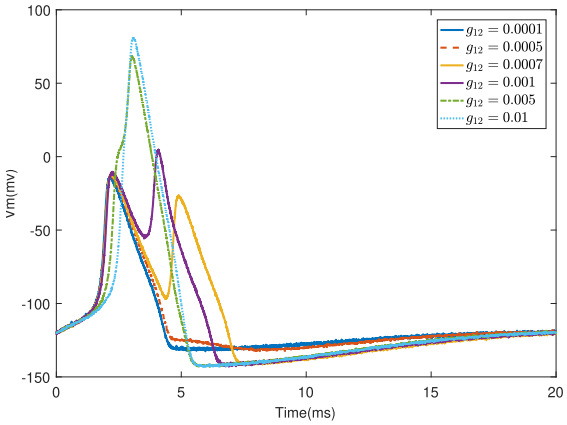

FIGURE 9. The measured data of the membrane voltage with standard Gaussian white noise.

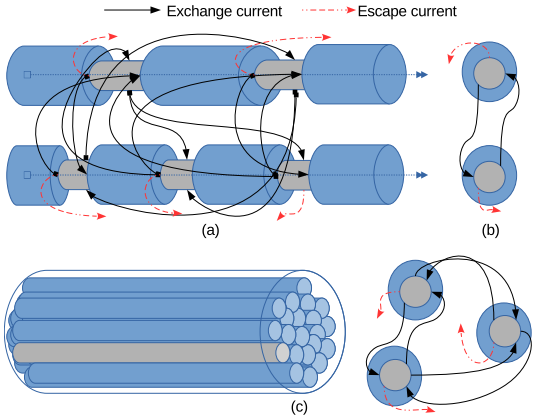

FIGURE 10. The interaction is complex even if we only considered two myelinated axons and these figures demonstrate the assumption in this paper. (a) The 3D mode illustrates the interaction between two myelinated axons while the interaction is also described by the exchange currents and the escape current. (b) The transverse mode shows that the multi-node interaction can be replaced by a statistical coupling factor matrix while the axons can be analysed by the equivalent two matched Ranvier nodes.(c) The multi-axon case is illustrated where the interactive activities can be characterised by the pairwise description based on the assumptions shown in (a) and (b).

micro-electrode array (MEA) [29], etc, the data set of the measured axons in this case can be described by

$$\bar{V}_{m,k} = \sum_{i=1}^{n} V_{m_i,k} + e_k \tag{38}$$

Thus the estimated measured membrane potential can be further expressed by

$$\hat{\bar{V}}_{m,k}\left(\hat{\Xi}\right) = \sum_{i=1}^{n} \hat{V}_{m_i,k} \tag{39}$$

Similar to the presented approach, the estimation error $\tilde{V}_k(\Xi)$ can be obtained and the coupling of the coupled axons can also be characterised following the presented iterative learning identification with the entropy-based performance criterion. The convergence for this estimation algorithm can be analysed similarly to the algorithm analysis in Section III. In order to demonstrate the effectiveness, we supply another numerical example as follows.

Suppose that we have two coupled axons, where the mutual coupling factor is a real constant g_{12}, the measured potential should be the sum of these two membrane potentials. Then the shapes of the measured potentials is dominated by the mutual coupling factor while the curves are shown below.

Similarly, the presented algorithm can be used for these measured data sets directly, and the performance criterion can also be calculated for each batch.

B. STATISTICAL DESCRIPTION OF THE INTERACTION BETWEEN NERVE FIBERS

Using the similar approach, the interaction can also be described by the exchange of the coupled membrane currents, where the escape current has to be taken into accounts and the mutual coupling factor should be extended from the view of statistic. Suppose that the influence of the interaction depends on the distance while it obeys Gaussian distribution. Therefore, the multi-node interaction among myelinated axons in this case can be equivalent to one statistical coupling factor matrix between pairwise axons (see Fig. 10). Based on this assumption, the interaction between multi-axon can be formulated as follows:

$$I_{i,k} = \left(1-\epsilon_{i,k}\right) I_{i,k-1} + \sum_{j=1}^{n} \gamma_{ij,k} \left(I_{j,k-1} - I_{i,k-1}\right), \quad j \neq i \tag{40}$$

where I stands for the membrane current. ϵ and γ denote the escape factor and the coupling factor of the membrane current at k-th Ranvier node, respectively. $i, j = 1, \ldots, n$ denote the indexes of the axons while the generalised coupling factor matrix Ξ_k is rewritten by the following expression.

$$\Xi_k = \begin{bmatrix} 1 - \epsilon_{1,k} - \sum \gamma_{1j,k} & \cdots & \gamma_{1n,k} \\ \vdots & \ddots & \vdots \\ * & \cdots & 1 - \epsilon_{n,k} - \sum \gamma_{nj,k} \end{bmatrix} \tag{41}$$

We define that $0 \leq \epsilon, \gamma < 0.5$ and Xi_k is symmetric matrix which means, for instance, the current amount with opposite directions from node 1 to node 2 is equal to the current from node 2 to node 1.

Therefore, the statistical descriptive model can be divided into two different layers based on the scale. As a result, the dynamic model of each individual myelinated axon among the nerve fibres can be given as follows:

$$\bar{I} = \bar{C}\frac{\partial V}{\partial t} + I_{ion} \tag{42}$$

where $\bar{I}$ is the membrane current without the influence of the interaction.

Next, the interactive activities can be described based on the static equation which combines the extended coupling

factor matrix.

$$I_k = \Xi_k \bar{I}_{k-1} \tag{43}$$

Notice that Ξ_k becomes the identify matrix if the escape factors and the coupling factors are 0. In this case, it implies that there is no interaction phenomena among the nerve fibres.

Remark 5.1: It has been shown that the presented model is equivalent to the standard Hodgkin-Huxley equation if Ξ_k is the identify matrix, then the dynamics of the membrane potential can be analysed individually.

Remark 5.2: Both the presented descriptive approaches from the view of voltage and current are equivalent because the current and voltage are linear and static in the extracellular environment.

C. THE CONDUCTION OF NERVE SIGNALS

Combining cable theory and Kirchhoff's current law, the extended model with the interaction can be concluded as follows:

$$I_{i,k} + G_a(2V_{in_i,k} - V_{in_i,k-1} - V_{in_i,k+1}) = 0 \tag{44}$$

where G_a denotes the internodal axial conductance.

Thus, the complete model can be restated as follows:

$$\begin{aligned} \tau_{i,k}\frac{\partial V_{m_i,k}}{\partial t} - \lambda_{i,k}^2 \frac{V_{m_i,k-1} - 2V_{m_i,k} + V_{m_i,k+1}}{\Delta s^2} \\ + V_{m_i,k} + \frac{1}{g_{l_{i,k}}}(\bar{\epsilon}_{i,k} i_{ion_{i,k}} + \sum_{j\neq i}^{n} \gamma_{ij,k}\bar{I}_{j,k}) \\ = \lambda_{i,k}^2 \frac{V_{out_i,k-1} - 2V_{out_i,k} + V_{out_i,k+1}}{\Delta s^2} \end{aligned} \tag{45}$$

where $\bar{\epsilon}_i := 1 - \epsilon_i - \sum_{j\neq i}^{n} \gamma_{ij}$, $V_m := V_{in} - V_{out} - V_r$ and g_l is the leakage conductance while the time constant and space constant for i-th axon can be calculated by

$$\tau_{i,k} = \sqrt{\frac{C_{m_{i,k}}}{G_{l_{i,k}}}}, \lambda_{i,k} = \sqrt{\frac{C_{a_{i,k}}}{\bar{\epsilon}_i G_{l_{i,k}}}}\Delta s \tag{46}$$

where Δs is the compartment length.

Noticed that when $\Delta s \to 0$, the model for the unmyelinated axons can be obtained directly by replacing the deference with the derivative.

$$\begin{aligned} \tau_{i,k}\frac{\partial V_{m_i,k}}{\partial t} - \lambda_{i,k}^2 \frac{\partial^2 V_{m_i,k}}{\partial s^2} + \frac{1}{g_{l_{i,k}}}(\bar{\epsilon}_{i,k} i_{ion_{i,k}} + \sum_{j\neq i}^{n} \gamma_{ij,k}\bar{I}_j) \\ + V_{m_i,k} = \lambda_{i,k}^2 \frac{\partial^2 V_{out_i,k}}{\partial s^2} \end{aligned} \tag{47}$$

Although further validation of the models is needed, a similar strategy can also be applied to scenarios including extracellular electrode, even multi-electrode arrays. Moreover, the finite element method [30] can be used as an extension for this model due to the fact that the presented coupling factor matrix is a static description and the basic structure of the model has not been changed, which is still a second-order partial differential equation.

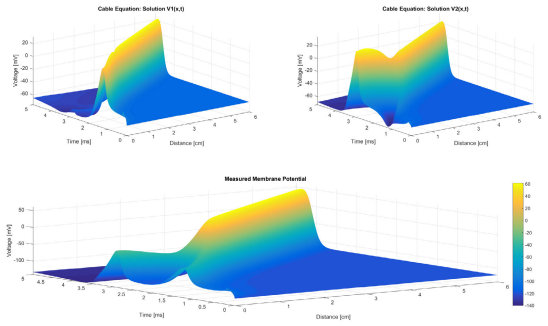

FIGURE 11. The information conduction of the coupled axons with coupling factor $\gamma = 0.4$.

Another benefit of using a statistical approach is that we do not consider the transient coupling influence on a piece of membrane. Basically, it is possible to add a coupling factor matrix in the dynamic equation. However, the dynamics of the membrane potential may become overly complex and all the signals would increase the randomness of the matrix. In other words, the exchange currents will be considered as a mutual noise. We cannot use the model with noise to develop any application and it cannot be used to characterise the interaction. Moreover, this statistical coupling description can be considered as an equivalent approach of the coupling coefficient in [31]. Furthermore, using this statistical approach, the interactive phenomena can be described through different observation scales.

As an example with two coupled axons, the following figure shows that the action potential would be achieved in coupled axon 2 even if only the axon 1 is stimulated. For any location along the axon, the responses of the these axons are same to the simulation results mentioned in Section IV. Moreover, the conduction of the neural signals are demonstrated by the 3D mesh. Generally, the electric field should be considered which slightly affects the extracellular potential of the membrane [32], however we chose the injected current as the stimulation and ignore the influence of the produced electric field.

D. ODE APPROXIMATION

Motivated by the measurement of the nerve signals, the concept of virtual neuron [19], [26] is presented to abstract the group behaviour of the axons with the neural couplings, while the potential of this virtual neuron can be approximated by the sum of these equivalent potentials of the axons. It is clear that we cannot use the single membrane potential model to describe the group behaviour, thus a simple ordinary differential equation (ODE) is used to estimate the behaviour of the virtual neuron.

$$\frac{\partial^2 V_{v,i}}{\partial t^2} + 2\eta_i \frac{\partial V_{v,i}}{\partial t} + \omega_i V_{v,i} = 0 \tag{48}$$

Furthermore, the estimated V can be obtained by

$$\hat{V}_{v,i} = V_{v,i} - (n-1)V_r, \tag{49}$$

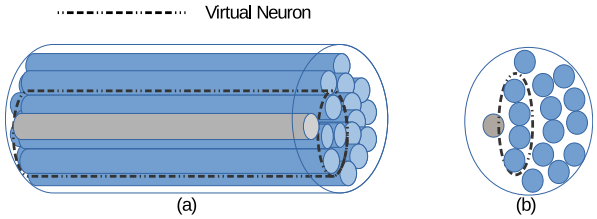

FIGURE 12. The simplified multi-axons within the neural tissue using the presented virtual neuron. (a) The 3D mode illustrates the virtual neuron. (b) The transverse mode shows how a virtual neuron can be abstracted from a 'wrapped up' group of axons in a distance dependent manner.

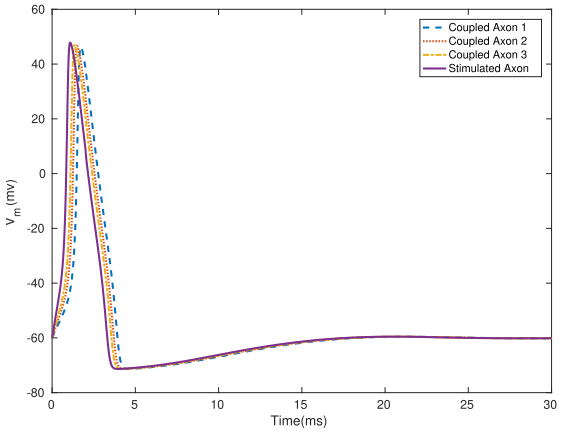

FIGURE 13. The responses of the multi-axons with $\gamma_1 = 0.15$, $\gamma_2 = 0.2$, $\gamma_3 = 0.25$ and $1mA/cm^2$ stimulation current.

where $\hat{V}_{v,i}$ denotes the potential of the virtual neuron in terms of the i-th axon. V_r denotes resting potential of neuron.

Notice that η_i and ω_i can be obtained by numerical approximation as follows:

$$\{\eta_i, \omega_i\} = argmin \mid \hat{V}_{v,i} - V_i \mid \tag{50}$$

Since the damping rate of the second order (ODE) is defined by $\xi_i = \eta_i/\omega_i$, then $\xi_i > 0$ can be calculated by η_i and ω_i as the coupling factor of the nerve group.

The influence of the interaction depends on the distance, which implies that some of the interactive activities can be neglected if the distance between the coupled axons is large enough. Based on this assumption, the interactive analysis of the coupled group behaviour can be reduced to the analysis of the subgroup (Fig.12).

The model we presented in this paper can be considered as as extension strategy of the existing membrane dynamic model. Based on virtual neuron, the interaction problem can be analysed simply as two axons with the mutual coupling factor. Notice that the optimal parametric searching for the ODE approximation can also use the presented iterative learning identification algorithm replacing the extended Hodgkin-Huxley model with the 2nd-order ordinary differential equation.

For example, the group behaviour can be described using the virtual neuron which can be formulated by the measurement of nerve signals. In the following figures, three coupled

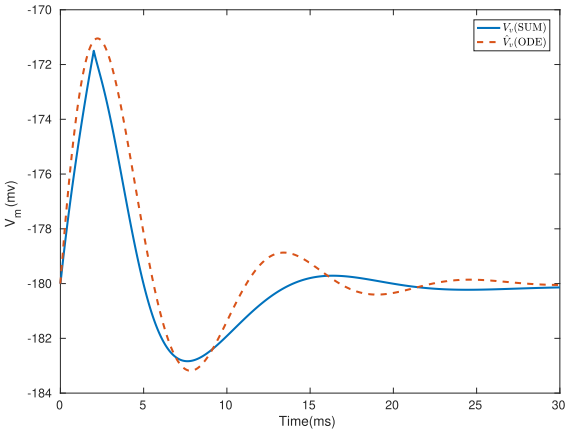

FIGURE 14. The estimation of group behaviour by ODE.

axons achieve action potentials and the measured signal is the sum of these potentials. Moreover, the curve of the measured potential can be approximated by the ODE with optimal parameters $\eta = 0.37$ and $\omega = 0.35$.

VI. CONCLUSION AND FUTURE WORKS

The interaction phenomena of the coupled axons has been investigated. In order to describe the mechanism of these interactions, the mutual coupling factor is presented as a pairwise description. Combining the famous Hodgkin-Huxley model and the coupling factor matrix, the quantified characterisation approach is presented by identify the coupling factors for the coupled myelinated/unmyelinated axons by analysing the dynamic of membrane potentials. Since the descriptive model is strong nonlinear, an entropy-based iterative learning estimation algorithm is developed where the selection of the learning rate has been analysed to guarantee the convergence of the operation. Meanwhile the presented model and algorithm are verified by the numerical simulation as well. All the results and the useful discussions demonstrate that the presented model and algorithm are effect and convenient to extend for some more complex cases. Finally, the novelties of this paper are summarised as follows: 1) The extended membrane potential model has been presented for the coupled axons rather than individual axon; 2) A novel convergent iterative learning algorithm is proposed to characterise the neural iteration; 3) Based on the presented model, couples of potential extensions have been discussed such as the concept of virtual neuron, the measurement/conduction of nerve signals.

For applications, the coupled nerve signals are quite difficult to reproduce while the interaction also leads to a complex signal analysis therefore the stimulation currents can be designed properly to attenuate the neural interaction which can be considered as the neural decoupling. On the other hand, the spike rate would be affected due to these interactions. Thus the statistical model of the spike rate can be investigated which is very significant problem for neural encoding and decoding. In addition, considering the

uncertainties between various data batches, the process can be further modelled following Markov jump form, then the adaptive strategy for batch-to-batch learning can be extended using the framework in [33], [34].

APPENDIX A
PROOF OF LEMMA 3.1

Proof: According to property of the convergence, the sub performance criterion has to be decrease function along with the batches d, which leads to

$$\mathscr{H}\left(\tilde{V}_d\left(\hat{\Xi}_d\right)\right) < \mathscr{H}\left(\tilde{V}_{d-1}\left(\hat{\Xi}_{d-1}\right)\right) \tag{51}$$

Then we have

$$\log_b \mathscr{P}\left(\tilde{V}_d\left(\hat{\Xi}_d\right)\right) > \log_b \mathscr{P}\left(\tilde{V}_{d-1}\left(\hat{\Xi}_{d-1}\right)\right) \tag{52}$$

which means that

$$\log_b\left(\frac{\mathscr{P}\left(\tilde{V}_d\left(\hat{\Xi}_d\right)\right)}{\mathscr{P}\left(\tilde{V}_{d-1}\left(\hat{\Xi}_{d-1}\right)\right)}\right) > 0 \tag{53}$$

Since b can be selected as $0 < b < 1$, the inequality can be rewritten by

$$\frac{\mathscr{P}\left(\tilde{V}_d\left(\hat{\Xi}_d\right)\right)}{\mathscr{P}\left(\tilde{V}_{d-1}\left(\hat{\Xi}_{d-1}\right)\right)} < 1 \tag{54}$$

Notice that the information potential is always non-negative, then the inequality can further expressed by

$$\mathscr{P}\left(\tilde{V}_{d-1}\left(\hat{\Xi}_{d-1}\right)\right) > \mathscr{P}\left(\tilde{V}_d\left(\hat{\Xi}_d\right)\right) \geq 0 \tag{55}$$

which implies that the convergence should be resulted in the following condition.

$$\frac{\partial \mathscr{P}\left(\tilde{V}_{d-1}\left(\hat{\Xi}_{d-1}\right)\right)}{\partial d} < 0 \tag{56}$$

Substituting the kernel density estimation, then we have

$$\begin{aligned}
&\frac{\partial}{\partial d}\left(\frac{1}{(k\bar{h})^2}\sum_{i=1}^{k}\left[\sum_{j=1}^{k} G_\sigma\left(\frac{\tilde{V}_{d-1,j}-\tilde{V}_{d-1,i}}{\bar{h}}\right)\right]^2\right)\\
&= \frac{2}{(k\bar{h})^2}\sum_{i=1}^{k}\left\{\sum_{j=1}^{k} G_\sigma\left(\frac{\tilde{V}_{d,j}-\tilde{V}_{d,i}}{\bar{h}}\right)\right.\\
&\quad\left.\times\left[\sum_{j=1}^{k}\frac{\partial}{\partial \tilde{V}_d} G_\sigma\left(\frac{\tilde{V}_{d-1,j}-\tilde{V}_{d-1,i}}{\bar{h}}\right)\frac{\partial \Delta}{\partial d}\right]\right\}\\
&= \frac{2}{\sigma^2\sqrt{2\pi}(k\bar{h})^2\bar{h}}\sum_{i=1}^{k}\left\{\sum_{j=1}^{k} G_\sigma\left(\frac{\tilde{V}_{d-1,j}-\tilde{V}_{d-1,i}}{\bar{h}}\right)\right.\\
&\quad\left.\times\left[\sum_{j=1}^{k}\exp\left(\frac{-\left(\tilde{V}_{d-1,j}-\tilde{V}_{d-1,i}\right)^2}{2(\sigma\bar{h})^2}\right)\Delta\frac{\partial \Delta}{\partial d}\right]\right\}
\end{aligned} \tag{57}$$

where

$$\begin{aligned}
\Delta &= \tilde{V}_{d-1,j} - \tilde{V}_{d-1,i}\\
\frac{\partial \Delta}{\partial d} &= \frac{\partial \tilde{V}_{d-1,i}}{\partial d} - \frac{\partial \tilde{V}_{d-1,j}}{\partial d}
\end{aligned} \tag{58}$$

Note that $\tilde{V}_{d-1,i}$ and $\tilde{V}_{d-1,i}$ denote the elements of the vector $\tilde{V}_{d-1}$. Thus there always exist two real positive number M_d and N_d such that the following inequalities hold.

$$\begin{aligned}
\frac{\partial \Delta}{\partial d} &\leq \sup\left(\frac{\partial \tilde{V}_{d-1}}{\partial d}\right) - \inf\left(\frac{\partial \tilde{V}_{d-1}}{\partial d}\right)\\
&< M_d \sup\left(\frac{\partial \tilde{V}_{d-1}}{\partial d}\right)
\end{aligned} \tag{59}$$

$$\Delta \leq \sup\left(\tilde{V}_{d-1}\right) - \inf\left(\tilde{V}_{d-1}\right) < N_d \sup\left(\tilde{V}_{d-1}\right) \tag{60}$$

where $\sup(\cdot)$ and $\inf(\cdot)$ stand for the supremum and infimum operations.

Moreover, since the estimation error is bounded and dominated by the estimated coupling factor, we can also claim that there exists a real positive number $\bar{M}_d$ then the following inequality holds.

$$\frac{\partial \tilde{V}_{d-1}}{\partial d} \leq \bar{M}_d \frac{\partial \Xi_{d-1}}{\partial d}\bigg|_{\Xi_{d-1}=\hat{\Xi}_{d-1}} \tag{61}$$

Using the iterative learning formula (22), the inequality above can be rewritten as

$$\frac{\partial \tilde{V}_{d-1}}{\partial d} \leq \varepsilon_d \bar{M}_d \frac{\partial J_{d-1}}{\partial \Xi_{d-1}} \tag{62}$$

Substituting Eq.(59) - Eq.(62) into Eq.(57), the following condition can be obtained to satisfy the inequality (57) since $G_\sigma(\cdot)$ is Gaussian distribution function.

$$\bar{N}_d \sup\left(\tilde{V}_{d-1}\right) \sup\left(\varepsilon_d \frac{\partial J_{d-1}}{\partial \Xi_{d-1}}\right) < 0 \tag{63}$$

where $\bar{N}_d = N_d M_d \bar{M}_d > 0$ and the condition (28) can be obtained which completes the proof. ■

APPENDIX B
PROOF OF LEMMA 3.2

Proof: According to property of the convergence, the sub performance criterion needs to be decrease function along with the batches d, which leads to

$$\mathscr{E}\left(\tilde{V}_d^T\left(\hat{\Xi}_d\right)\tilde{V}_d\left(\hat{\Xi}_d\right) - \tilde{V}_{d-1}^T\left(\hat{\Xi}_{d-1}\right)\tilde{V}_{d-1}\left(\hat{\Xi}_{d-1}\right)\right) < 0 \tag{64}$$

This inequality can be restated by

$$\begin{aligned}
&\hat{\tilde{V}}_d^T\left(\hat{\Xi}_d\right)\hat{\tilde{V}}_d\left(\hat{\Xi}_d\right) - \hat{\tilde{V}}_{d-1}^T\left(\hat{\Xi}_{d-1}\right)\hat{\tilde{V}}_{d-1}\left(\hat{\Xi}_{d-1}\right)\\
&\quad - 2\bar{V}^T\left(\hat{\tilde{V}}_d\left(\hat{\Xi}_d\right) - \hat{\tilde{V}}_{d-1}\left(\hat{\Xi}_{d-1}\right)\right) < 0
\end{aligned} \tag{65}$$

Notice that $\hat{\tilde{V}}_{d-1}^T\left(\hat{\Xi}_{d-1}\right)\hat{\tilde{V}}_{d-1}\left(\hat{\Xi}_{d-1}\right)$ is always positive then the inequality above can be further expressed as

$$\hat{\tilde{V}}_d^T\left(\hat{\Xi}_d\right)\hat{\tilde{V}}_d\left(\hat{\Xi}_d\right) < 2\bar{V}^T\left(\hat{\tilde{V}}_d\left(\hat{\Xi}_d\right) - \hat{\tilde{V}}_{d-1}\left(\hat{\Xi}_{d-1}\right)\right) \tag{66}$$

The estimated membrane potential vector can be further expressed by the following equation substituting the discrete-time format of the model.

$$\hat{\bar{V}}_d\left(\hat{\Xi}_d\right) = \Big[\hat{\bar{V}}_{d,1}^T, \hat{\bar{V}}_{d,1}^T + t_s\bar{f}^T\left(\hat{\bar{V}}_{d,1}, \hat{\Xi}_d, I_{ap}\right), \ldots, \hat{\bar{V}}_{d,1}^T + t_s\sum_{i=1}^{k-1}\bar{f}^T\left(\hat{\bar{V}}_{d,i}, \hat{\Xi}_d, I_{ap}\right)\Big]^T \quad (67)$$

This expression results in the following inequality.

$$\begin{aligned}\hat{\bar{V}}_d^T\left(\hat{\Xi}_d\right)\hat{\bar{V}}_d\left(\hat{\Xi}_d\right) &= k\hat{\bar{V}}_{d,1}^T\hat{\bar{V}}_{d,1} \\ &+ 2t_s\hat{\bar{V}}_{d,1}^T\sum_{j=1}^{k-1}\sum_{i=1}^{j}\bar{f}\left(\hat{\bar{V}}_{d,i}, \hat{\Xi}_d, I_{ap}\right) \\ &+ t_s^2\sum_{j=1}^{k-1}\sum_{i=1}^{j}\bar{f}^T\left(\hat{\bar{V}}_{d,i}, \hat{\Xi}_d, I_{ap}\right)\bar{f}\left(\hat{\bar{V}}_{d,i}, \hat{\Xi}_d, I_{ap}\right) \quad (68)\end{aligned}$$

Note that the first elements of each batch data vectors are equal to each other which is denoted by

$$\hat{\bar{V}}_{d,1} = \hat{\bar{V}}_{d-1,1} \quad (69)$$

Thus, we have

$$\begin{aligned}&\bar{V}^T\left(\hat{\bar{V}}_d\left(\hat{\Xi}_d\right) - \hat{\bar{V}}_{d-1}\left(\hat{\Xi}_{d-1}\right)\right) \\ &= \bar{V}^T\Big[0, t_s\left(\bar{f}\left(\hat{\bar{V}}_{d,1}, \hat{\Xi}_d, I_{ap}\right) - \bar{f}\left(\hat{\bar{V}}_{d-1,1}, \hat{\Xi}_{d-1}, I_{ap}\right)\right), \\ &\quad \ldots, t_s\sum_{i=1}^{k-1}\left(\bar{f}\left(\hat{\bar{V}}_{d,i}, \hat{\Xi}_d, I_{ap}\right) - \bar{f}\left(\hat{\bar{V}}_{d-1,i}, \hat{\Xi}_{d-1}, I_{ap}\right)\right)\Big] \\ &= t_s\sum_{j=1}^{k-1}\sum_{i=1}^{j}\bar{V}_{j+1}^T\Big(\bar{f}\left(\hat{\bar{V}}_{d,i}, \hat{\Xi}_d, I_{ap}\right) \\ &\quad -\bar{f}\left(\hat{\bar{V}}_{d-1,i}, \hat{\Xi}_{d-1}, I_{ap}\right)\Big) \quad (70)\end{aligned}$$

To simply the expression, we use $f_{d,i}$ to denote the function $f\left(\hat{\bar{V}}_{d,i}, I_{ap}\right)$, the inequity (66) can be rewritten by

$$\begin{aligned}&k\hat{\bar{V}}_{d,1}^T\hat{\bar{V}}_{d,1} - 2t_s\hat{\bar{V}}_{d,1}^T\bar{C}\sum_{j=1}^{k-1}\sum_{i=1}^{j}\left(\bar{I}_{d,i} + \Xi_d\left(f_{d,i} - \hat{\bar{V}}_{d,i}\right)\right) \\ &\quad + t_s^2\bar{C}^T\bar{C}\sum_{j=1}^{k-1}\sum_{i=1}^{j}\Big(\bar{I}_{d,i}^T\bar{I}_{d,i} + 2I_{d,i}^T\Xi_d\left(f_{d,i} - \hat{\bar{V}}_{d,i}\right) \\ &\quad + \left(f_{d,i} - \hat{\bar{V}}_{d,i}\right)^T\Xi_d^T\Xi_d\left(f_{d,i} - \hat{\bar{V}}_{d,i}\right)\Big) \\ &< 2t_s\sum_{j=1}^{k-1}\sum_{i=1}^{j}\bar{V}_{j+1}^T\Big(\bar{C}\bar{I}_{d-1,i} + \bar{C}\,\Xi_{d-1}\left(f_{d-1,i} - \hat{\bar{V}}_{d-1,i}\right) \\ &\quad - \bar{C}\bar{I}_{d,i} - \bar{C}\,\Xi_d\left(f_{d,i} - \hat{\bar{V}}_{d,i}\right)\Big) \quad (71)\end{aligned}$$

Substituting the iterative learning formula, the condition (30) can be given and the proof can be completed. ■

ACKNOWLEDGMENT

The authors would like to thank the editor and the reviewers for their valuable comments which improve the quality of this article. Qichun Zhang would also like to thank Prof. F. Sepulveda, University of Essex, U.K., for the discussions about the neural membrane modeling, this is acknowledged.

REFERENCES

[1] G. Buzsáki, C. A. Anastassiou, and C. Koch, "The origin of extracellular fields and currents—EEG, ECOG, LFP and spikes," *Nature Rev. Neurosci.*, vol. 13, no. 6, pp. 407–420, 2012.
[2] A. L. Hodgkin and A. F. Huxley, "A quantitative description of membrane current and its application to conduction and excitation in nerve," *J. Physiol.*, vol. 117, no. 4, p. 500, 1952.
[3] B. Frankenhaeuser and A. Huxley, "The action potential in the myelinated nerve fibre of xenopus laevis as computed on the basis of voltage clamp data," *J. Physiol.*, vol. 171, no. 2, p. 302, 1964.
[4] S. E. Grossberg, *Neural Networks and Natural Intelligence*. Cambridge, MA, USA: MIT Press, 1988.
[5] S. Martinoia, P. Massobrio, M. Bove, and G. Massobrio, "Cultured neurons coupled to microelectrode arrays: Circuit models, simulations and experimental data," *IEEE Trans. Biomed. Eng.*, vol. 51, no. 5, pp. 859–863, May 2004.
[6] J. W. Clark and R. Plonsey, "A mathematical study of nerve fiber interaction," *Biophysical J.*, vol. 10, no. 10, pp. 937–957, Oct. 1970.
[7] L. Ljung, *System Identification*. Hoboken, NJ, USA: Wiley, 1999.
[8] H. Wang and P. Afshar, "ILC-based fixed-structure controller design for output PDF shaping in stochastic systems using LMI techniques," *IEEE Trans. Autom. Control*, vol. 54, no. 4, pp. 760–773, Apr. 2009.
[9] S. He, H. Fang, M. Zhang, F. Liu, X. Luan, and Z. Ding, "Online policy iterative-based H∞ optimization algorithm for a class of nonlinear systems," *Inf. Sci.*, vol. 495, pp. 1–13, Aug. 2019.
[10] S. He, H. Fang, M. Zhang, F. Liu, and Z. Ding, "Adaptive optimal control for a class of nonlinear systems: The online policy iteration approach," *IEEE Trans. Neural Netw. Learn. Syst.*, vol. 31, no. 2, pp. 549–558, Feb. 2020.
[11] Q. Zhang and F. Sepulveda, "Entropy-based axon-to-axon mutual interaction characterization via iterative learning identification," in *Proc. EMBEC & NBC*. Singapore: Springer, 2017, pp. 691–694.
[12] Q. Zhang and X. Dai, "Entropy-based iterative learning estimation for stochastic non-linear systems and its application to neural membrane potential interaction," in *Proc. 1st Int. Conf. Ind. Artif. Intell. (IAI)*, Jul. 2019, pp. 1–6.
[13] S. Raspopovic, M. Capogrosso, F. M. Petrini, M. Bonizzato, J. Rigosa, G. Di Pino, and J. Carpaneto, "Restoring natural sensory feedback in real-time bidirectional hand prostheses," *Sci. Transl. Med.*, vol. 6, no. 222, p. 222ra19, 2014.
[14] F. Kolbl, M. C. Juan, and F. Sepulveda, "Impact of the angle of implantation of transverse intrafascicular multichannel electrodes on axon activation," in *Proc. IEEE Biomed. Circuits Syst. Conf. (BioCAS)*, Oct. 2016, pp. 484–487.
[15] X. Tang, Q. Zhang, and L. Hu, "An EKF-based performance enhancement scheme for stochastic nonlinear systems by dynamic set-point adjustment," *IEEE Access*, vol. 8, pp. 62261–62272, 2020.
[16] Q. Zhang and L. Hu, "Probabilistic decoupling control for stochastic nonlinear systems using EKF-based dynamic set-point adjustment," in *Proc. UKACC 12th Int. Conf. Control (CONTROL)*, Sep. 2018, pp. 330–335.
[17] X. Yin, Q. Zhang, H. Wang, and Z. Ding, "RBFNN-based minimum entropy filtering for a class of stochastic nonlinear systems," *IEEE Trans. Autom. Control*, vol. 65, no. 1, pp. 376–381, Jan. 2020.
[18] Q. Zhang, "Performance enhanced Kalman filter design for non-Gaussian stochastic systems with data-based minimum entropy optimisation," *AIMS Electron. Electr. Eng.*, vol. 3, no. 4, p. 382, 2019.
[19] Q. Zhang and F. Sepulveda, "A statistical description of pairwise interaction between nerve fibres?" in *Proc. 8th Int. IEEE/EMBS Conf. Neural Eng. (NER)*, May 2017, pp. 194–198.
[20] H. Wang, "Minimum entropy control of non-Gaussian dynamic stochastic systems," *IEEE Trans. Autom. Control*, vol. 47, no. 2, pp. 398–403, Aug. 2002.
[21] T. M. Cover and J. A. Thomas, *Elements of Information Theory*. Hoboken, NJ, USA: Wiley, 2012.

[22] M. Ren, Q. Zhang, and J. Zhang, "An introductory survey of probability density function control," *Syst. Sci. Control Eng.*, vol. 7, no. 1, pp. 158–170, Jan. 2019.
[23] J. C. Principe, *Information Theoretic Learning: Rényi's Entropy and Kernel Perspectives*. New York, NY, USA: Springer, 2010.
[24] Q. Zhang and A. Wang, "Decoupling control in statistical sense: Minimized mutual information algorithm," *Int. J. Adv. Mech. Syst.*, vol. 7, no. 2, pp. 61–70, 2016.
[25] F. Rattay, "The basic mechanism for the electrical stimulation of the nervous system," *Neuroscience*, vol. 89, no. 2, pp. 335–346, Mar. 1999.
[26] Q. Zhang and F. Sepulveda, "A model study of the neural interaction via mutual coupling factor identification," in *Proc. 39th Annu. Int. Conf. IEEE Eng. Med. Biol. Soc. (EMBC)*, Jul. 2017, pp. 3329–3332.
[27] H. Brown and D. DiFrancesco, "Voltage-clamp investigations of membrane currents underlying pace-maker activity in rabbit sino-atrial node," *J. Physiol.*, vol. 308, p. 331, Nov. 1980.
[28] K. D. Wise, J. B. Angell, and A. Starr, "An integrated-circuit approach to extracellular microelectrodes," *IEEE Trans. Biomed. Eng.*, vol. BME-17, no. 3, pp. 238–247, Jul. 1970.
[29] G. W. Gross, E. Rieske, G. W. Kreutzberg, and A. Meyer, "A new fixed-array multi-microelectrode system designed for long-term monitoring of extracellular single unit neuronal activity *in vitro*," *Neurosci. Lett.*, vol. 6, nos. 2–3, pp. 101–105, Nov. 1977.
[30] H. Meffin, B. Tahayori, D. B. Grayden, and A. N. Burkitt, "Modeling extracellular electrical stimulation: I. Derivation and interpretation of neurite equations," *J. Neural Eng.*, vol. 9, no. 6, Dec. 2012, Art. no. 065005.
[31] Q. Zhang, J. Zhou, H. Wang, and T. Chai, "Minimized coupling in probability sense for a class of multivariate dynamic stochastic control systems," in *Proc. 54th IEEE Conf. Decis. Control (CDC)*, Dec. 2015, pp. 1846–1851.
[32] S. Joucla and B. Yvert, "Improved focalization of electrical microstimulation using microelectrode arrays: A modeling study," *PLoS ONE*, vol. 4, no. 3, p. e4828, Mar. 2009.
[33] S. He, M. Zhang, H. Fang, F. Liu, X. Luan, and Z. Ding, "Reinforcement learning and adaptive optimization of a class of Markov jump systems with completely unknown dynamic information," *Neural Comput. Appl.*, vol. 32, pp. 1–10, Apr. 2019.
[34] P. Cheng, J. Wang, S. He, X. Luan, and F. Liu, "Observer-based asynchronous fault detection for conic-type nonlinear jumping systems and its application to separately excited DC motor," *IEEE Trans. Circuits Syst. I, Reg. Papers*, vol. 67, no. 3, pp. 951–962, Mar. 2020.

XIAFEI TANG received the B.Eng. degree in electrical engineering and automation from Beihang University, in 2006, and the Ph.D. degree in electrical and electronic engineering from The University of Manchester, U.K., in 2012. After that, she joined the Changsha University of Science in 2013. She is currently working as a Lecturer with the School of Electrical and Information Engineering. Her research interests include disturbance rejection, nonlinear systems control, the stability analysis of power systems, and risk assessment of power systems.

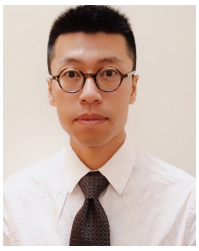

QICHUN ZHANG (Senior Member, IEEE) received B.Eng. degree in automation and the M.Sc. degree in control theory and control engineering from Northeastern University, China, in 2008 and 2010, respectively, and the Ph.D. degree in electrical and electronic engineering from The University of Manchester, U.K., in 2016. He is currently a Lecturer of computer science with the University of Bradford, U.K. Before joining Bradford, he was a Senior Lecturer of dynamics and control with De Montfort University, a Senior Research Officer of neural engineering with the University of Essex, and an Academic Visitor with the Control Systems Center, The University of Manchester. He also serves over 20 international journals as an Active Reviewer. His research interests include stochastic dynamic systems, probabilistic coupling analysis, decoupling control, performance optimisation, brain–computer interface, and computational modeling for peripheral nervous systems. He is an Associate Editor of IEEE Access and *Journal of Intelligent Manufacturing*. He is also an Academic Editor of *PLOS One*, *PeerJ Computer Science*, and an Editorial Board member for other four journals.

XUEWU DAI (Member, IEEE) received the B.Eng. degree in electronic engineering and the M.Sc. degree in computer science from Southwest University, China, in 1999 and 2003, respectively, and the Ph.D. degree in electronic and electrical engineering from The University of Manchester, U.K., in 2008. He is currently a Senior Lecturer with the Department of Mathematics, Physics and Electrical Engineering, Northumbria University. His research interests include robust state estimation and condition monitoring, networked control systems, wireless sensor actuator networks, and industrial Internet of Things. His research interests also include wireless sensor networks, media access control, system identification, filtering and fault detection for industrial process and gas turbine engine condition monitoring, and fuzzy neural networks and optimisation. He is also interested in field-bus-based distributed control systems and networked control systems.

YIQUN ZOU received the B.Eng. degree in automation from Tianjin University, Tianjin, China, in 2004, and the Ph.D. degree in control engineering from The University of Manchester, Manchester, U.K., in 2010. He is currently an Associate Professor with the School of Automation, Central South University. His current research interests include system identification, optimisation, and target localisation.